

A remarkable, precisely timed release of hyperglycemic hormone from endocrine cells in the gut is associated with ecdysis in the crab *Carcinus maenas*

J. Sook Chung*, Heinrich Dirksen†, and Simon G. Webster**

*School of Biological Sciences, University of Wales, Bangor, Gwynedd, LL57 2UW, United Kingdom; and †Institut für Zoophysiologie, University of Bonn, Endenicher Allee 11-13, D-53115 Bonn, Germany

Edited by John H. Law, University of Arizona, Tucson, AZ, and approved September 17, 1999 (received for review June 10, 1999)

Molting or ecdysis is the most fundamentally important process in arthropod life history, because shedding of the exoskeleton is an absolute prerequisite for growth and metamorphosis. Although the hormonal mechanisms driving ecdysis in insects have been studied extensively, nothing is known about these processes in crustaceans. During late premolt and during ecdysis in the crab *Carcinus maenas*, we observed a precise and reproducible surge in hemolymph hyperglycemic hormone (CHH) levels, which was over 100-fold greater than levels seen in intermolt animals. The source of this hormone surge was not from the eyestalk neurosecretory tissues but from previously undescribed endocrine cells (paraneurons), in defined areas of the foregut and hindgut. During premolt (the only time when CHH is expressed by these tissues), the gut is the largest endocrine tissue in the crab. The CHH surge, which is a result of an unusual, almost complete discharge of the contents of the gut endocrine cell, regulates water and ion uptake during molting, thus allowing the swelling necessary for successful ecdysis and the subsequent increase in size during postmolt. This study defines an endocrine brain/gut axis in the arthropods. We propose that the ionoregulatory process controlled by CHH may be common to arthropods, in that, for insects, a similar mechanism seems to be involved in antidiuresis. It also seems likely that a cascade of very precisely coordinated release of (neuro) hormones controls ecdysis.

In insects, preecdysial behavior, ecdysis, and subsequent associated events—such as air swallowing, hemolymph redistribution, and postecdysial behavior—are controlled by a complex, precisely timed interaction of several neuropeptides, including ecdysis-triggering hormone, eclosion hormone, and crustacean cardioactive peptide (1–6). Although analogous ecdysis-related events and behaviors must occur in crustaceans, nothing is known about the hormonal regulation of these processes in these arthropods. In spite of the large size of many decapod crustaceans in relation to other arthropods, which might be deemed a useful feature for physiological research, molting in most large, heavily calcified, adult decapod crustaceans is an annual event. Unlike insects, there are few obvious established behaviors or morphological events (7) useful in predicting ecdysis with the essential precision needed to elucidate the involvement of (neuro) hormones in this process. Nevertheless, during ecdysis in the green shore crab *Carcinus maenas*, we noticed increases in levels of circulating crustacean hyperglycemic hormone (CHH) immunoreactivity during the initial stages of ecdysis, culminating in a dramatic but transient (≈ 10 – 30 min) hormone surge and declining to basal values on completion of ecdysis. Although this neuropeptide is well known to be involved in energy mobilization in crustaceans (8) and more recently was reported to be involved in inhibition of ecdysteroid and juvenoid biosynthesis (9–11), we reasoned that this pattern of CHH release, which is very precisely temporally correlated with ecdysis (rupture of the epimeral lines and swelling), must be important in some aspect

of this process. Herein, we describe the temporal pattern of release of an authentic CHH, which is identical to that expressed by the eyestalk neurosecretory tissues from gut endocrine cells during ecdysis. The source of this hormone (previously undescribed paraneurons) and its action in stimulating water uptake at this time, which is necessary to allow ecdysis and subsequent swelling to postmolt dimensions, are also described.

Materials and Methods

Animals. Specimens of premolt *Carcinus maenas* were collected locally and maintained in a circulating seawater system under ambient conditions of temperature and photoperiod. Preparation for molt was staged by using the appearance and opening of the posteriolateral epimeral line and emergence from the old cuticle as visual markers. Other parameters for molt staging were based on established criteria (12).

Radioimmunoassay (RIA), Blood Chemistry, and Immunohistochemistry. RIA for CHH and CHH precursor-related peptide (CPRP) was performed by using ^{125}I -labeled peptides and polyclonal antisera (raised in rabbits by using HPLC-purified sinus gland peptides or, in the case of CPRP, by using a bovine thyroglobulin-peptide conjugate) essentially as described (13). Detection limits for both peptides in the assays used were below 0.5 fmol per tube. Peptides were extracted from snap-frozen (liquid N_2) hemolymph and tissue extracts by using Sep-Pak C_{18} cartridges (Waters), elution with 40% (vol/vol) isopropanol, and vacuum centrifugation (yields were routinely 70% CHH and 90% CPRP with this procedure). Hemolymph glucose and lactate levels were estimated as described (13). Whole-mount immunohistochemistry of foregut and hindgut was performed by using established protocols (14), and immunoreactive cells were visualized by using FITC or peroxidase-antiperoxidase/diaminobenzidine. For electron microscopic work, whole-mount peroxidase-antiperoxidase/diaminobenzidine-stained tissue fragments (showing immunopositive cells) were postfixed in 1% OsO_4 in 0.05 M sodium cacodylate (pH 7.4) containing 1.5% (vol/vol) $\text{K}_3\text{Fe}(\text{CN})_6$, dehydrated, embedded in Spurr's resin, sectioned, and counterstained with uranyl acetate/lead citrate.

PCR. Reverse transcription-PCR was performed on gut RNA isolated by using TRIzol (GIBCO/BRL), and 0.1- to 1- μg

This paper was submitted directly (Track II) to the PNAS office.

Abbreviations: CHH, crustacean hyperglycemic hormone; RIA, radioimmunoassay; CPRP, CHH precursor-related peptide; MALDI-TOF, matrix-assisted laser desorption ionization time-of-flight.

[‡]To whom reprint requests should be addressed. E-mail s.g.webster@bangor.ac.uk.

The publication costs of this article were defrayed in part by page charge payment. This article must therefore be hereby marked "advertisement" in accordance with 18 U.S.C. §1734 solely to indicate this fact.

quantities of RNA were reverse transcribed by using AMV reverse transcriptase (Roche Molecular Biochemicals) and cDNA amplified by using the following CHH gene-specific primers: forward 5'-GCCATGCTAGCAATCATCACCGTAG and reverse 5'-GTTGAGATCTGTTGTTTACTTTCC. After denaturation at 94°C for 4 min, PCR was done for 30 cycles consisting of denaturation at 94°C for 1 min, annealing at 55°C for 1 min, and extension for 72°C for 2 min. The amplification was terminated by a final extension at 72°C for 7 min. For a positive control, RNA extracted from the medulla terminalis of the eyestalk was used. Products were electrophoresed on 1.2% agarose gels with ethidium bromide visualization. PCR products of expected size (421 bp) were purified (Hybaid PCR purification kit, Middlesex, U.K.) and cloned in Top 10F' cells by using a TOPO-TA cloning kit (Invitrogen); positive clones were then sequenced.

HPLC and Mass Spectrometry. Sep-Pak purified hemolymph and gut extracts were fractionated by HPLC by using the following conditions: 300- × 3.9-mm Phenyl column (Waters), 1 ml·min⁻¹ gradient elution, 30–80% solvent B over 1 h [solvent A was 0.11% trifluoroacetic acid; solvent B was 60% (vol/vol) acetonitrile/0.1% trifluoroacetic acid]. Matrix-assisted laser desorption ionization time-of-flight (MALDI-TOF) mass spectrometry was performed on a Micromass Tofspec-E instrument (Micromass, Manchester, U.K.).

Radiography. Molt-staged crabs (beginning of ecdysis: stage E₁) were injected with CHH (100 pmol) or saline (controls) and immersed for 30 min in a stirred 20% (vol/vol) barium sulfate suspension in seawater, followed by rinsing and radiography, (X-protector, PLH Medical, Watford, U.K.) for 0.4 s by using Agfa CURIX PR1 x-ray film.

Results

During late premolt (stage D₄), levels of circulating CHH rapidly increased from typically low levels observed during intermolt (1–5 fmol/100 μl) to around 25 fmol/100 μl. During ecdysis (stage E), a consistent pattern of very dramatically increased levels of CHH was observed, with peak levels (150–200 fmol/100 μl) occurring during the latter stages of ecdysis (E_{50–100}). Immediately (within 1 h) after ecdysis, levels of CHH returned to basal values (Fig. 1A). With regard to the general time scale of ecdysis, the duration of stage D₄ is 4–24 h; that of initial swelling E_{1–30} is 200–500 min (in experimentally manipulated animals; see Fig. 4); E₃₀ to completion of ecdysis lasts 15–20 min. The source of CHH during this hormone surge was not from the eyestalk neurosecretory tissues, because animals whose stalks had been removed had identical patterns of CHH titer during ecdysis (and molted viably). Screening a variety of tissue extracts (including brain, stomatogastric ganglia, thoracic ganglia, gills, gonads, muscle, hepatopancreas, and gut) for CHH immunoreactivity during premolt revealed that the gut exclusively synthesized large quantities of CHH immunoreactive material during premolt. Immunoreactive content declined rapidly just before the dramatic increase in immunoreactive material in the hemolymph (Fig. 1A).

The immunoreactive material in the hemolymph during ecdysis (in crabs with and without eyestalks) was deemed to be authentic CHH on the basis of cochromatography by HPLC, of parallel dilution characteristics in RIA, and of mass determinations (MALDI-TOF) of HPLC-purified material eluting at the same time as sinus gland-derived CHH, which gave molecular ions corresponding to the Na⁺ (8,545 Da) and K⁺ (8,561 Da) salts of CHH. Additionally, CPRP, a 38-residue polypeptide of unknown function, which is part of the preprocessed CHH molecule (15, 16), was also detected in the hemolymph during the CHH surge.

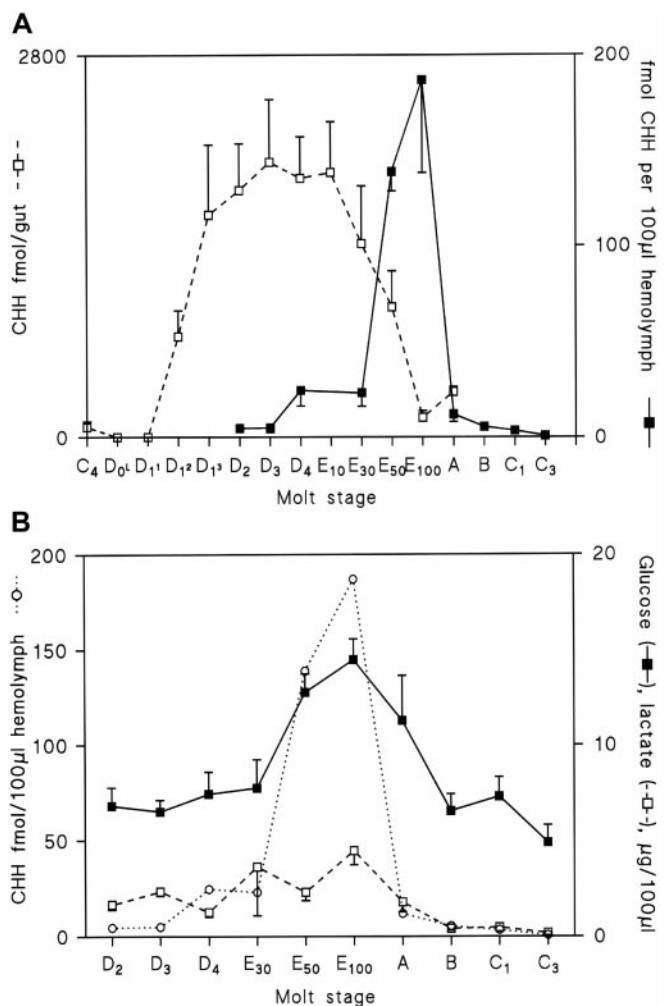


Fig. 1. CHH immunoreactivity in the hemolymph and gut tissues during the molt cycle and corresponding levels of glucose and lactate. (A) RIA analysis of hemolymph and gut tissue extracts. (B) Glucose and lactate levels during ecdysis ($n = 5-10$ estimations; means \pm SEM for each point). Mean CHH titers shown in A have been included for reference. Molt stages were assigned by using established criteria based on morphogenesis of setae during premolt and cuticle flexibility during postmolt (12). During ecdysis (stage E), the percentage of emergence from the old cuticle was used for quantification of molt. Although the highest levels of circulating CHH were apparently observed at 100% ecdysis, the variability seen at this time, coupled with low levels of CHH observed during immediate postmolt (stage A, within 1 h of molting), suggested that peak CHH levels occurred shortly after stage E₅₀.

The immunoreactive material in gut extracts was deemed authentic by cochromatography (HPLC) with sinus gland-derived CHH (Fig. 2A and B) and by MALDI-TOF [molecular ions corresponding to the Na⁺ (8,545 Da) and K⁺ (8,561 Da) salts were identified from HPLC purified premolt gut extract eluting at the retention time of CHH]. Reverse transcription-PCR of premolt gut total RNA with gene-specific primers based on the prepro-CHH nucleotide sequence (15) gave an amplified product identical in size to that obtained from eyestalk tissue (Fig. 2C). Sequencing of the product revealed complete identity with the nucleotide sequence and conceptual amino acid sequence of prepro-CHH from the eyestalk and CPRP (15, 16), which were identical in these respects to one of the three CPRPs produced by the eyestalk neurosecretory system of *Carcinus* (J.S.C. and S.G.W., unpublished results). During ecdysis, levels of glucose and lactate increased only marginally and fell to intermolt levels within 24 h of molting (Fig. 1B).

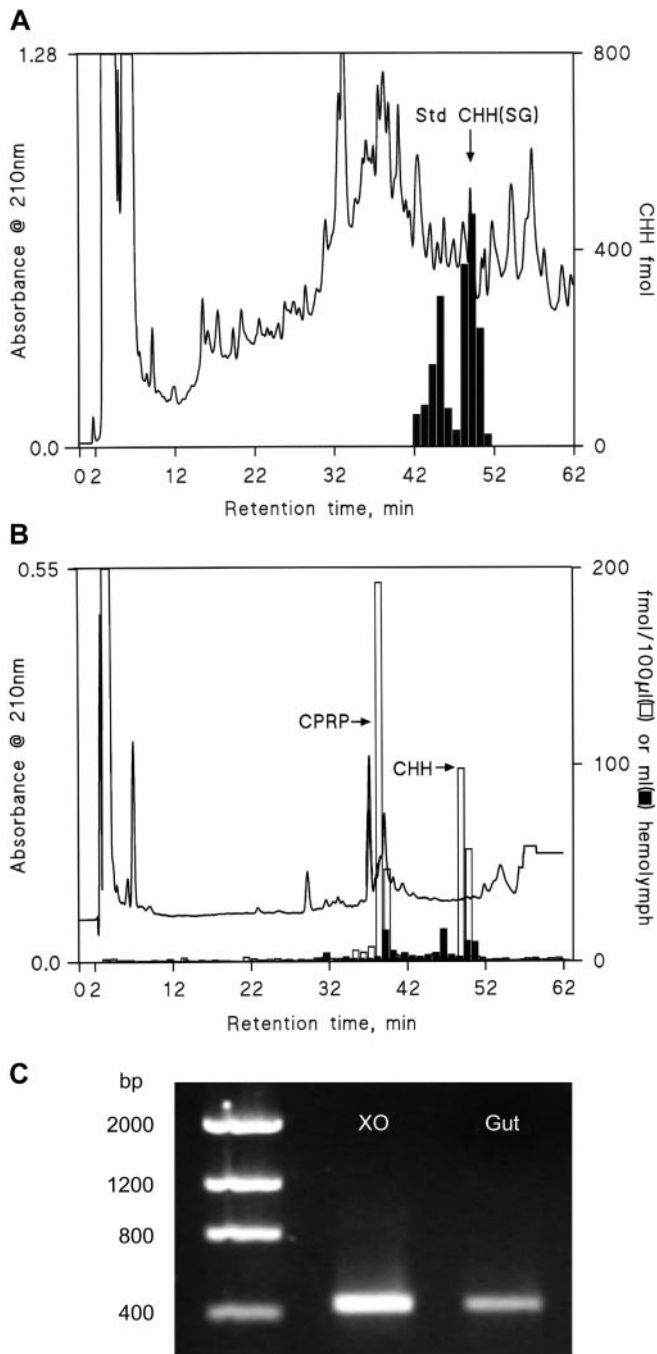


Fig. 2. Identification of CHH in hemolymph and tissue extracts. (A) RIA analysis of fractions from HPLC separation (HPLC RIA) of Sep-Pak purified premolt (stage D₄–E₃₀) hemolymph. The arrow indicates retention time of authentic CHH. (B) HPLC RIA identification of hemolymph extracts from crabs without eyestalks in intermolt (10 ml; stage C₄; n = 5; filled bars) and premolt (13 ml; stage E₅₀; n = 8; open bars). The arrows indicate retention times of authentic CHH and CPRP. (C) Reverse transcription–PCR of total RNA derived from premolt X organs of the eyestalk (XO) and gut tissues. The amplified (421-bp) gut PCR product was cloned and sequenced and was identical to the previously sequenced XO prohormone cDNA sequence (15).

Whole-mount immunohistochemistry of *Carcinus* guts revealed many thousands of endocrine cells, which were immunopositive to antisera raised against both CHH and CPRP (Fig. 3A–D). These cells were found only in the chitin-lined foregut and hindgut; cells were never observed in the midgut or asso-

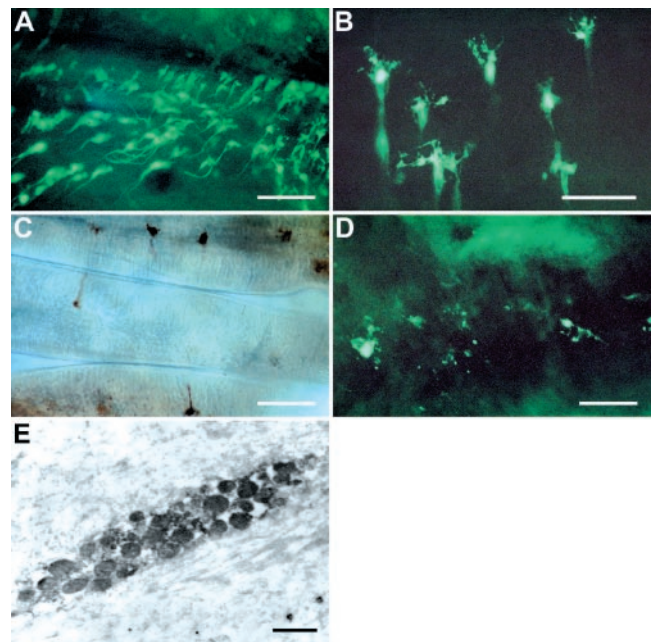


Fig. 3. Immunohistochemistry of gut endocrine cells. (A) Whole-mount FITC preparation of the posterior margin of the pyloric ampulla of the stomach (stage D₂) showing a band of abundant CHH immunoreactive cells. (B) This image is similar to A but shows fine detail of cells; in particular, note the fine arborizations facing the hemocoelic side of the ampulla. (C) Peroxidase-antiperoxidase-immunostained whole mount of the hindgut (CPRP antiserum), showing a low but uniform distribution of immunoreactive cells closely associated with longitudinal muscle fibers. View from hemocoelic face of hindgut. In all cases, cells were immunopositive for both CHH and CPRP. (D) FITC-stained whole mount of the same region of the pyloric ampulla shown in A and B from a postmolt (stage A) crab. Note sparse immunoreactivity, poorly defined cells, and the presence of immunoreactive material (possibly cell debris) on the hemocoelic face of the ampulla. (E) Ultrathin section of a peroxidase-antiperoxidase/diaminobenzidine-stained whole mount, which was treated with OsO₄ to increase electron density of the immunoreactive granules. CHH immunoreactive cell from the pyloric ampulla. (Bars = 100 µm for A, C, and D; 50 µm for B; 250 nm for E.)

ciated diverticulae. Large numbers of cells were associated with the anteroventral and posteriolateral margins of the pyloric ampullae and were most abundant in gut epithelia adjacent to muscle insertions, particularly the external and internal inferior pyloric dilator muscles (17). In the hindgut, the immunoreactive cells were scattered but appeared mainly confined to infoldings of the gut lumen adjacent to the longitudinal muscles. The cells had a very distinctive morphology, including an extensive array of arborizations abutting the hemocoelic spaces and a narrow ($\approx 10 \mu\text{m}$) tapering cell body terminating at the chitinous surface of the gut. The nuclei were invariably located at the widest part of the cells adjacent to the arborizations. At the ultrastructural level, the cells contained many dense-cored vesicles ($\approx 125\text{--}150 \text{ nm}$ in diameter; Fig. 3E). To date, detailed examination of these cells has proved difficult. When regions of the gut (pyloric ampullae) were examined immediately after molting, very few immunoreactive cells could be observed. Thus, it seems that the surge in hormone titer seen during ecdysis was accompanied by an almost complete secretion of hormone content of these cells (Fig. 3D). Additionally, the hemocoelic side of the gut was often littered with immunoreactive cell debris, suggestive of cell death.

To determine the function of the CHH hormone surge during ecdysis, crabs at very precisely staged periods of ecdysis were injected with CHH (100 pmol). This procedure resulted in a marked acceleration of ecdysis, the magnitude of which was related to the stage at which animals were injected (Fig. 4). For

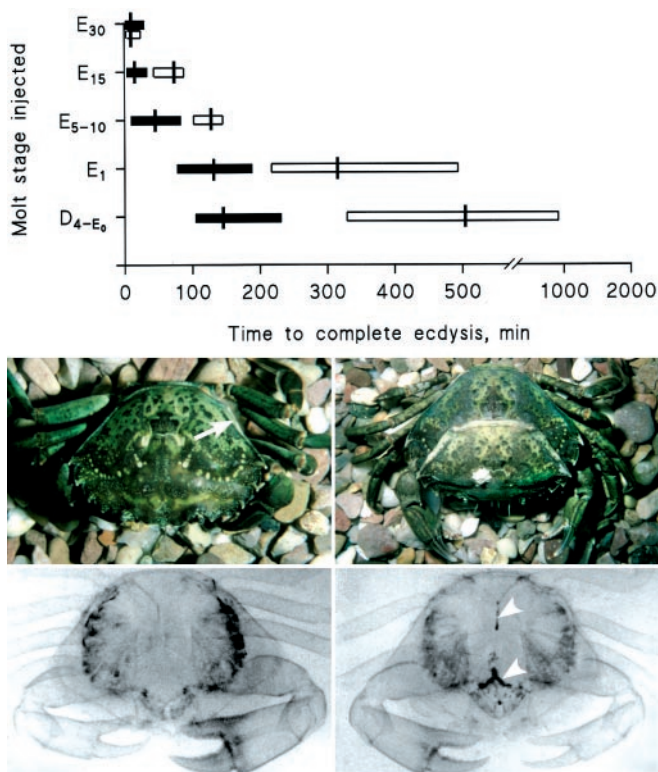


Fig. 4. CHH initiates ecdysis. The graph shows the effect of a single injection of 100 pmol CHH (filled bars) on the time to complete ecdysis compared to that of saline injections (open bars) when administered during D₄ and early ecdysial (E₁₋₃₀) stages. Vertical bars indicate means; horizontal bars indicate ranges ($n = 3-10$ crabs for each measurement). The photographs show the effect of a single injection of 300 pmol CHH during molt stage E₁ (Upper Right), which results in the rapid uptake of water 2 h after injection, compared to a saline-injected control (5 h after injection; Upper Left); the arrow indicates the epimeral suture line. In the hormone-injected crab, the old carapace (note barnacle) is being shed, and the crab has swollen abnormally, which subsequently prevented successful ecdysis. (Lower) Radiograms of a crab injected with 100 pmol CHH (Lower Right) and a saline-injected crab (Lower Left) immersed in 15% (vol/vol) barium sulfate in seawater, 30 min after injection. Note radiopaque areas indicating accumulation of barium sulfate in the pyloric ampullae and hindgut in the hormone-injected crab (arrowheads), indicative of drinking and water absorption. Radiopaque dark lateral areas represent barium sulfate trapped in gill tissues. This material was difficult to remove in control crabs, whereas, in hormone injected crabs, the impending molt allowed efficient rinsing of the gills.

example, injection at the beginning of ecdysis (stage D₄-E₀) reduced the mean time taken to complete ecdysis from 500 min to 140 min. Injection of CHH during later stages of ecdysis (E₁₅) reduced the mean time to ecdysis from 60 min to 10 min. If larger doses of CHH were injected, ecdysis was always unsuccessful, judging by the fact that the legs of the crabs became trapped in the exoskeleton because of a very marked and abnormal swelling. Radiography of crabs injected with CHH (Fig. 4) revealed that hormone-induced swelling was associated with accumulation of barium sulfate in the stomach and anterior hindgut, indicating dramatic increases in seawater drinking and, in consequence, water absorption.

Discussion

In this study, we have shown that ecdysis in *Carcinus maenas* is associated with a precisely timed surge in circulating CHH levels, which is a result of an unusual, almost complete release of this hormone from a previously undescribed endocrine tissue, namely the gut. The endocrine cells in the foregut and hindgut

responsible for this hormone surge possess a very similar morphology to previously described endocrine cells of the insect gut (18, 19) or the “closed” type of paraneuron described by Fujita *et al.* (20), although these cells clearly differ from previously described “putative” endocrine cells from the crustacean midgut (21). Furthermore, no immunopositive cells were seen in this region of the gut. In view of the very distinctive morphology of these cells, reminiscent of the habitus of *Hydra*, we propose that they be called “hydroid cells.” During intermolt, these cells are not visible by immunohistochemical techniques but, during premolt (in accord with the RIA results), the cells become strongly immunoreactive. However, after molting, very little immunoreactivity was observed, except for some cell debris, which suggested that the CHH surge was a result of almost complete secretion of peptide contents, if not cell death. In this context, it is of interest to note that complete secretion of cellular peptide content has been observed in insect (nonneuronal) epitracheal “Inka cells” after the ecdysis-triggering hormone surge before eclosion (1) and the dramatic release of eclosion hormone from proctodeal nerves before eclosion (22). Thus, parallels might perhaps be drawn concerning this unusual mode of complete peptide release for functionally critical hormones during ecdysis in the arthropods.

What is the function of the CHH surge? Because ecdysis is very energy demanding and possibly stressful, an obvious role for CHH at this time might be in regulation of stress-related hyperglycemia (8). However, during ecdysis, blood glucose levels show only a moderate increase, and hypoxia (as evidenced by increased blood lactate levels) is slight (Fig. 1B). Because ecdysis in crustaceans depends on a very impressive uptake of water via the gut (23, 24), it seemed possible that the CHH surge was in some way linked to this phenomenon. When crabs were injected with physiologically relevant (100 pmol) quantities of CHH before the expected endogenous CHH surge, we observed a precocious initiation of significant uptake of water (swelling), which resulted in accelerated ecdysis, relative to saline-injected controls (Fig. 4). When higher levels (300 pmol) of CHH were injected, swelling was very rapid; in addition, molting was unsuccessful, because the crab became trapped in the old exoskeleton of the legs because of the enormous tissue expansion.

At present, we do not know the precise mechanisms by which CHH increases water uptake. Increased drinking is involved, as evidenced from barium meal radiographic experiments (Fig. 4). An ionoregulatory action of CHH is also plausible. Because seawater drinking is inevitably associated with preecdysial swelling, which occurs in an organism essentially isosmotic with its external environment, active uptake of salts across the gut epithelia followed by passive movement of water seems likely. It has long been known, from ultrastructural and physiological studies, that the hindgut and midgut are highly osmotically active (23) and that these tissues are predominantly responsible for water and ion uptake during molting (24). It is known that in locusts, hindgut (ileal) chloride transport is stimulated by an ion transport peptide, which, by activating electrogenic Cl⁻ pumps, can drive isosmotic fluid reabsorption by the ileum (25-27). Because this peptide (which was the first insect member of the CHH peptide family to be isolated) is highly structurally related to *Carcinus* CHH (39% sequence identity), an attractive hypothesis would be one involving similar ionic mechanisms that drive (isosmotic) water uptake by the hindgut in crustaceans. The CHH-containing cells of the foregut and hindgut seem ideally placed to detect changes in gut tension. In particular, the cells at the anteroventral margin of the pyloric ampullae, associated with the external and internal inferior pyloric dilator muscles, may be influenced (mechanically) by changes in the pyloric motor rhythm at ecdysis. In lobsters (*Homarus gammarus*), a deep preecdysial hypoxia modulates motor network expression

of the stomatogastric ganglion (28). Our preliminary results on changes in oxygen tension in the hemolymph in *Carcinus* during ecdysis (J.S.C. and S.G.W., unpublished results) and the rather moderate increases in blood lactate seen at this time (Fig. 1B) suggest that deep preecdysial hypoxia does not occur in *Carcinus* (as would befit a well adapted intertidal crustacean). However, it is entirely possible that a mechanically stimulated release of CHH from these cells during ecdysis could act locally on the gut and centrally in circulation. Indeed, perfusion of the circulatory system with India ink to reveal the fine structure of the arterial circulatory system has shown that the pyloric ampullae, in particular, have a very impressive arterial microcapillary blood supply (J.S.C. and S.G.W., unpublished results). If the proposed scenario were correct, then, strikingly, a common mechanism would control disparate functions: antidiuresis (insects) and ecdysial swelling (crustaceans). Nevertheless, CHH is certainly not the only neuropeptide that is involved in crustacean molting. Crustacean cardioactive peptide (29) is intimately involved in stereotyped eclosion behavior in insects (6), and evidence is now accumulating showing that release of crustacean cardioactive peptide into the hemolymph at precisely defined times during the

later stages of ecdysis controls stereotyped ecdysial behavior in crustaceans (31, 32). Additionally, because expression of CHH in gut endocrine cells during premolt closely follows increases in ecdysteroid levels during this period, it is likely that activation of transcription of CHH genes in these cells may be mediated by ecdysteroids. Obviously, the early (swelling) and subsequent (behavioral) processes during ecdysis must be tightly temporally regulated to culminate in successful molting. To paraphrase the statements of Truman (2) and Hesterlee and Morton (31), many more layers of complexity, which remain to be shed, still shroud the remarkable phenomenon of molting in crustaceans.

We are grateful to A. Tweedale for providing a continuous supply of crabs, D. A. Davies for imaging work and software advice, D. J. Grove (Ocean Sciences, Menai Bridge, U.K.) for use of radiographic facilities, R. S. Thorpe for the underwater photography, C. Kowalczyk (Biological Sciences, Sussex, U.K.) for performing the MALDI-TOF mass spectrometry, and A. Rosin (Genetics, Liverpool, U.K.) for DNA sequencing. This work was supported by a Natural Environment Research Council grant to S.G.W. and grants from the German Academic Exchange Service (DAAD-ARC program) to H.D.

1. Žitnán, D., Kingan, T. G., Hermesman, J. L. & Adams, M. E. (1996) *Science* **271**, 88–91.
2. Truman, J. W. (1996) *Science* **271**, 40–41.
3. Gammie, S. C. & Truman, J. W. (1997) *J. Neurosci.* **17**, 4389–4397.
4. Ewer, J., Gammie, S. C. & Truman, J. W. (1997) *J. Exp. Biol.* **200**, 869–881.
5. Kingan, T. G., Gray, W., Žitnán, D. & Adams, M. E. (1997) *J. Exp. Biol.* **200**, 3425–3426.
6. Gammie, S. C. & Truman, J. W. (1999) *J. Exp. Biol.* **202**, 343–352.
7. Reynolds, S. E. (1980) *Adv. Insect Physiol.* **15**, 475–595.
8. Keller, R. (1992) *Experientia* **48**, 439–448.
9. Van Herp, F. (1998) in *Advances in Arthropod Endocrinology*, eds. Coast, G. M. & Webster, S. G. (Cambridge Univ. Press, Cambridge, U.K.), pp. 53–70.
10. Chung, J. S. & Webster, S. G. (1996) *Eur. J. Biochem.* **240**, 358–364.
11. Liu, L. & Laufer, H. (1996) *Arch. Insect Biochem. Physiol.* **32**, 375–381.
12. Drach, P. & Tchernigovtzeff, C. (1967) *Vie Milieu Ser A* **18**, 595–607.
13. Webster, S. G. (1996) *J. Exp. Biol.* **199**, 1579–1585.
14. Dirksen, H., Müller, A. & Keller, R. (1991) *Cell Tissue Res.* **263**, 439–457.
15. Weidemann, W., Gromoll, J. & Keller, R. (1989) *FEBS Lett.* **257**, 31–34.
16. Tensen, C. P., Verhoven, A. H. M., Gaus, G., Janssen, K. P. C., Keller, R. & Van Herp, F. (1991) *Peptides* **12**, 673–681.
17. Maynard, D. M. & Dando, M. R. (1974) *Philos. Trans. R. Soc. London* **268**, 162–219.
18. Montuenga, L. M., Barrenechea, M. A., Sesma, P., Lopez, T. & Vazquez, J. J. (1989) *Cell Tissue Res.* **258**, 577–583.
19. Žitnán, D., Šauman, I. & Sehnal, F. (1993) *Arch. Insect Biochem. Physiol.* **22**, 113–132.
20. Fujita, T., Kanno, T. & Kobayashi, S. (1988) *The Paraneuron* (Springer, Tokyo).
21. Mykles, D. L. (1979) *Zoomorphology* **92**, 201–215.
22. Hewes, R. S. & Truman, J. W. (1991) *J. Comp. Physiol. A* **168**, 697–707.
23. Mykles, D. L. (1980) *J. Exp. Biol.* **84**, 89–101.
24. Malley, D. F. (1977) *J. Exp. Biol.* **70**, 231–245.
25. Audsley, N., McIntosh, C. & Phillips, J. E. (1992) *J. Exp. Biol.* **173**, 275–288.
26. Phillips, J. E. & Audsley, N. (1995) *Am. Zool.* **35**, 503–514.
27. Meredith, J., Ring, M., Macins, A., Marschall, J., Cheng, N. N., Theilmann, D., Brock, H. W. & Phillips, J. E. (1996) *J. Exp. Biol.* **199**, 1053–1061.
28. Clemens, S., Massabuau, J.-C., Meyrand, P. & Simmers, J. (1999) *J. Exp. Biol.* **202**, 817–827.
29. Stangier, J., Hilbich, C. & Keller, R. (1987) *Proc. Natl. Acad. Sci. USA* **84**, 575–589.
30. Johnen, C., von Gliscynski, U. & Dirksen, H. (1995) *Neth. J. Zool.* **45**, 38–40.
31. Phlippen, M. K., Webster, S. G., Chung, J. S. & Dirksen, H. (1999) *J. Exp. Biol.*, in press.
32. Hesterlee, S. & Morton, D. B. (1996) *Curr. Biol.* **6**, 648–650.